Journal of Geoscience and Environment Protection, 2026, 14(6), 1-22
https://www.scirp.org/journal/gep
ISSN Online: 2327-4344
ISSN Print: 2327-4336

The Impact and Mechanisms of Different ENSO Types on the Interannual Variability of Summer Dry-Hot Events in Mauritania

Eida Savi[1,2], Liwei Huo[1,2]

[1]State Key Laboratory of Climate System Prediction and Risk Management/Key Laboratory of Meteorological Disaster, Ministry of Education/Collaborative Innovation Center on Forecast and Evaluation of Meteorological Disasters, Nanjing University of Information Science and Technology, Nanjing, China
[2]School of Atmospheric Sciences, Nanjing University of Information Science and Technology, Nanjing, China
Email: eydeqlf@gmail.com

How to cite this paper: Savi, E., & Huo, L. W. (2026). The Impact and Mechanisms of Different ENSO Types on the Interannual Variability of Summer Dry-Hot Events in Mauritania. *Journal of Geoscience and Environment Protection, 14,* 1-22.
https://doi.org/10.4236/gep.2026.146001

Received: April 30, 2026
Accepted: June 12, 2026
Published: June 15, 2026

Abstract

Understanding the drivers of compound dry-hot extremes is crucial for climate risk assessment in the Sahel, a region highly vulnerable to hydroclimatic variability. This study investigates the interannual variability and mechanisms of summer (June-September, JJAS) compound dry-hot events over Mauritania during 1979-2025, with particular focus on the distinct roles of preceding spring Eastern Pacific (EP) and Central Pacific (CP) ENSO types. A Probability Index (PI), derived from the joint probability density function of temperature and precipitation, is employed to characterize compound events. Empirical Orthogonal Function (EOF) analysis reveals two dominant modes: EOF1 (51.29% variance) exhibits a spatially coherent country-wide pattern in which negative PI anomalies correspond to more severe compound dry-hot conditions, while EOF2 (16.51%) displays a pronounced north-south dipole. Further analysis establishes that PC1 is significantly correlated with the EP ENSO index ($r = 0.55$, $p < 0.001$), while PC2 is significantly correlated with the CP ENSO index ($r = 0.38$, $p < 0.05$). Mechanistically, EP-type El Niño induces widespread Walker circulation-driven subsidence, suppressed convection, reduced atmospheric moisture, and surface warming across the entire country. CP-type El Niño produces a meridionally asymmetric response with subsidence in the south and anomalous ascent in the north, generating the observed dipole pattern. These results highlight the importance of distinguishing ENSO diversity in understanding and predicting compound climate extremes in the Sahel.

Keywords

Probability Index, Mauritania, EP and CP ENSO Types, Dry-Hot Events, Compound Climate Extremes, Interannual Variability, Sahelian Climate

1. Introduction

Compound dry-hot events defined as periods of concurrent precipitation deficits and extreme high temperatures represent one of the most devastating categories of climate extremes, with profound consequences for agriculture, water resources, public health, and ecosystem stability (Nicholson, 2005; Giannini et al., 2008). Their combined impacts substantially exceed those of individual drought or heatwave events because simultaneous stressors overwhelm the coping capacity of natural and human systems. Over recent decades, compound dry-hot events have increased in frequency and intensity across many regions globally, driven largely by anthropogenic climate change and rising greenhouse gas concentrations (IPCC, 2021; Diffenbaugh et al., 2017). The Intergovernmental Panel on Climate Change (IPCC) Sixth Assessment Report warns that the risk of compound extremes will continue to grow substantially under all future emission scenarios, with particularly severe projected increases in arid and semi-arid regions of Africa (IPCC, 2021).

Mauritania, situated in the western Sahel (15˚N - 27˚N, 5˚W - 17˚W), represents one of the world's most climate-vulnerable nations. The country straddles the transition between the hyper-arid Sahara Desert to the north and the semi-arid Sahelian savanna to the south, making it highly sensitive to West African Monsoon (WAM) variability. The WAM governs the short but critically important summer rainy season (JJAS; June-September), during which Mauritania receives the vast majority of its annual precipitation (Giannini et al., 2008). Historical records document catastrophic Sahel droughts in the 1970s and 1980s that resulted in widespread famine, mass displacement, and substantial socioeconomic losses (Nicholson, 2005). Although a partial recovery of Sahelian rainfall has been observed since the late 1990s, the region remains highly vulnerable to interannual climate variability. The combination of poverty, rain-fed agriculture as the primary livelihood, inadequate infrastructure, and limited adaptive capacity means that even moderate deviations from normal climatic conditions can trigger humanitarian crises in Mauritania. Dry-hot extremes are particularly destructive because they simultaneously reduce crop yields through heat stress and soil moisture deficits, deplete water resources, increase livestock mortality, elevate the risk of wildfires, and drive public health emergencies through heat-related illness and food insecurity (Tabari & Willems, 2023).

The El Niño-Southern Oscillation (ENSO), arising from the coupled interaction between the tropical Pacific Ocean and the atmosphere, is the dominant driver of interannual climate variability on a global scale (Trenberth, 1997). ENSO modulates the climate of West Africa, particularly the Sahel, through both tropical and extratropical teleconnection pathways (Rowell, 2001; Joly & Voldoire, 2009). During El Niño events, the Walker circulation is weakened, suppressing convection over the Atlantic sector and West Africa, thereby reducing monsoon rainfall and increasing surface temperatures through anomalous subsidence and reduced cloud cover (Giannini et al., 2003; Janicot et al., 1996). La Niña events generally produce opposite effects, enhancing Sahelian rainfall and moderating temperatures. The strength and consistency of these ENSO teleconnections over the Sahel have made ENSO the primary basis for seasonal climate forecasts in the region (Rowell, 2001).

A critical advance in ENSO science over the past two decades has been the recognition that ENSO is not a monolithic phenomenon but encompasses at least two distinct types. The classical Eastern Pacific (EP) El Niño is characterized by maximum SST anomalies in the eastern equatorial Pacific (Niño3 region: 150˚W - 90˚W). The Central Pacific (CP) El Niño variously termed El Niño Modoki (Ashok et al., 2007), warm pool El Niño (Kug et al., 2009), or dateline El Niño (Larkin & Harrison, 2005), exhibits maximum SST anomalies in the central equatorial Pacific near the dateline. The CP type has increased in frequency since the 1990s and is projected to become more prevalent under future warming (Cai et al., 2014; Lee & McPhaden, 2010). These two types produce markedly different global teleconnection patterns, with distinct Rossby wave trains and differential regional climate impacts (Preethi et al., 2015; Ren & Jin, 2011; Kao & Yu, 2009). The EP type generally produces a stronger Rossby wave train across the North Atlantic, more strongly influencing West African climate, while the CP type generates a weaker but differently phased response with potentially distinct regional signatures (Preethi et al., 2015).

Despite this growing recognition of ENSO diversity, the differential effects of EP and CP ENSO on compound dry-hot events over Mauritania remain poorly understood. Most prior studies have focused exclusively on precipitation variability, neglecting the compounding role of simultaneous temperature anomalies (Zhang et al., 2023; Nicholson, 2013). Furthermore, the majority of studies treat ENSO as a single phenomenon, potentially obscuring distinct teleconnection pathways and physical mechanisms. The dynamic (vertical motion, wind anomalies) and thermodynamic (moisture transport, radiative effects) mechanisms by which different ENSO types modulate compound extremes in this region remain largely uncharacterized. This study addresses these gaps by employing a Probability Index (PI) framework, EOF analysis, and regression diagnostics to systematically characterize compound dry-hot event variability and link it to EP and CP ENSO over 1979-2025. The structure of the paper is as follows: Section 2 describes the study area, datasets, and methods; Section 3 presents results covering climatology, EOF modes, circulation anomalies, ENSO-PI linkages, and physical mechanisms; Section 4 provides conclusions and recommendations.

2. Data and Methods

2.1. Study Area

This study focuses on Mauritania (**Figure 1**), situated between 15˚N - 27˚N and 5˚W - 17˚W. The country shares its northern border with Algeria and Western

Sahara, eastern and southern borders with Mali, and its western boundary is delineated by the North Atlantic Ocean (754 km coastline). Mauritania occupies a critical transitional zone between the Sahara Desert in the north and the Sahelian savanna in the south, characterized by three distinct climatic zones. The northern coastal zone near Nouadhibou is moderated by the cold Canary Current, with average temperatures ranging from 20˚C in winter to 26.5˚C in September and negligible rainfall (<30 mm·yr^{-1}). When the Harmattan the dry north-easterly wind blows from the desert interior, temperatures can spike to 37˚C - 38˚C. The interior Saharan zone, north of ~20˚N, experiences extreme aridity with summer temperatures frequently exceeding 40˚C - 42˚C and annual rainfall near 55 mm. The central-southern Sahelian transition zone, encompassing the capital Nouakchott and extending southward, receives 200 - 475 mm·yr^{-1} during JJAS under the WAM. Historical droughts in the 1970s-1980s devastated this region, underscoring the population's high sensitivity to compound dry-hot extremes. The country's predominantly rain-fed agricultural economy and limited institutional adaptive capacity make it an ideal and policy-relevant study domain.

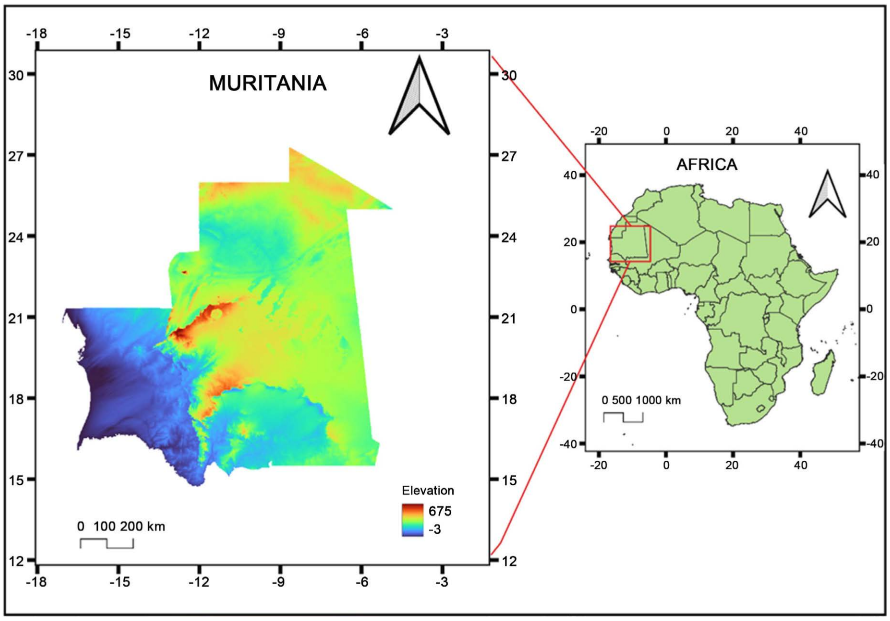

Figure 1. Location map of Mauritania showing the country's position within West Africa, Shading indicates elevation (m). The red rectangle denotes the study domain.

2.2. Data

Monthly atmospheric variables precipitation, zonal and meridional winds (u, v), vertical velocity (omega), geopotential height, specific humidity, outgoing longwave radiation (OLR), precipitable water vapor, and 2 m air temperature were obtained from the NCEP-NCAR Reanalysis 1 dataset (Kalnay et al., 1996) at 2.5˚ × 2.5˚ spatial resolution with 17 pressure levels (1000 - 10 hPa). Sea surface temperature (SST) data were derived from NOAA's ERSSTv5 dataset. While the NCEP-NCAR Reanalysis has a coarse spatial resolution (2.5˚ × 2.5˚) relative to the size of Mauritania, it remains the longest continuous reanalysis product covering the full study period (1979-2025) with complete global coverage. The reanalysis data is https://psl.noaa.gov/data/ gridded/data.ncep.reanalysis.html.

All variables were processed for the JJAS season, and seasonal total precipitation and seasonal mean values were calculated consistently. Long-term linear trends were removed from all variables prior to EOF and regression analyses to isolate interannual variability. All datasets underwent standard quality control procedures to ensure reliability and reproducibility.

2.3. Methods

Probability Index (PI). Following AghaKouchak et al. (AghaKouchak et al., 2014), the PI data used in this study was derived from the joint probability density function of total precipitation (P) and 2 m temperature (T 2 m) for the period 1979-2025 using an empirical copula approach using monthly ERA5 reanalysis data. The PI is a continuous index ranging from 0 to 1, with lower values indicating more severe compound dry-hot conditions (Salvadori et al., 2013; AghaKouchak et al., 2014).

In this study, a 'compound dry-hot event' is defined operationally at the seasonal timescale as a year in which the JJAS total precipitation falls below the 20th percentile of the historical distribution and the JJAS mean 2 m temperature exceeds the 80th percentile. This binary threshold-based definition complements the continuous Probability Index (PI) and ensures consistent terminology throughout the analysis.

Marginal distributions are estimated via the Weibull plotting position:

$$F_P\left(P_i\right)=\frac{r_i}{N+1}$$

And

$$F_T\left(t_i\right)=\frac{s_i}{N+1}$$

where s_i and r_i are the ranks of precipitation and temperature respectively and N is the sample size (Chow, 1964). The joint empirical copula is:

$$F_{P,T}\left(P_i,t_i\right)=\frac{1}{N}\sum_{j=1}^{N}1F_P(P_j)\le F_P(P_i),F_T\left(t_j\right)\le F_T\left(t_i\right)$$

The survival function for dry-hot events (low precipitation, high temperature) is

$$\bar{F}_{P,T}\left(P_i,t_i\right)=1-F_P\left(P_i\right)-F_T\left(t_i\right)+F_{P,T}\left(P_i,t_i\right)$$

Finally, the Probability Index (PI) is defined as:

$$PI=1-\bar{F}_{P,T}\left(P_i,t_i\right)=F_P\left(P_i\right)+F_T\left(t_i\right)-F_{P,T}\left(P_i,t_i\right)$$

From the above equation, the values of PI range from 0 to 1, with lower values indicating more severe compound dry-hot conditions (AghaKouchak et al., 2014; Salvadori et al., 2013). This empirical copula approach avoids parametric assumptions while capturing the full dependence structure between precipitation and temperature, making it particularly suitable for climate extremes analysis in data-sparse regions.

EOF Analysis. Empirical Orthogonal Function (EOF) analysis decomposes the spatiotemporal PI field into orthogonal spatial patterns and corresponding Principal Component (PC) time series (Hannachi et al., 2007). The PI field is first detrended to remove long-term trends and isolate interannual variability. The covariance matrix is computed from the anomaly field, and the eigenvalue problem is solved to yield EOFs ordered by explained variance. The significance of modes is assessed following the criterion in which cosine-latitude weighting was applied to account for the decreasing grid cell area toward the poles, following standard practice. The resulting PC time series are correlated with ENSO indices, such that positive PCs correspond to intensification of compound dry-hot events (low PI values) while the reverse holds for negative. Furthermore, the PCs were regressed onto atmospheric variables to identify the dynamical mechanisms governing each mode.

ENSO-Type Classification. The orthogonal indices of Ren and Jin (Ren & Jin, 2011) are employed:

$$N_{EP} = N3 - \alpha \times N4$$

$$N_{CP} = N4 - \alpha \times N3$$

where $\alpha = 2/5$ when ($N3 \times N4 \le 0$) and ($\alpha = 0$) otherwise, with $N3$ and $N4$ denoting the Niño3 and Niño4 indices. This piecewise linear transformation maximizes the separation between EP and CP ENSO events while maintaining near-zero mutual correlation ($r = -0.048$, $p > 0.05$ in this study), confirming orthogonality. The analysis uses the preceding spring (MAM) ENSO state, which exerts a lagged influence on summer climate through the persistence of Walker circulation anomalies and ocean-atmosphere memory. Statistical significance of correlations and regressions is evaluated using two-tailed Student's t-tests at 90%, 95%, and 99% confidence levels. Long-term trends are assessed using Sen's slope estimator and the Mann-Kendall test (Wilks, 2011).

3. Results and Discussion

3.1. Spatiotemporal Climatology and Trends

The JJAS PI climatology (1979-2025) reveals a distinct latitudinal gradient over Mauritania (**Figure 2**), with higher mean PI values (0.28 - 0.32) in the southern Sahelian zone and progressively lower values (0.16 - 0.18) northward into the arid Sahara. Since lower PI indicates more severe compound dry-hot conditions, this spatial pattern confirms that compound extremes are most intense in the northern Saharan zone, where persistent aridity and extreme temperatures combine throughout the year. The precipitation climatology shows monsoon rainfall concentrated in the south (250 - 350 mm·season^{-1}), declining sharply northward, forming the dominant meridional gradient that characterizes West African monsoon dynamics. 2 m temperature ranges from approximately 32˚C in the south to 43˚C in the northeast, with the highest values collocated with the driest regions where clear skies allow maximum surface radiative heating. The spatial distribution of the PI during JJAS is broadly consistent with both the precipitation and temperature fields, with the compound dry-hot event risk gradient reflecting the competing influences of WAM-supplied moisture in the south and persistent arid conditions in the north.

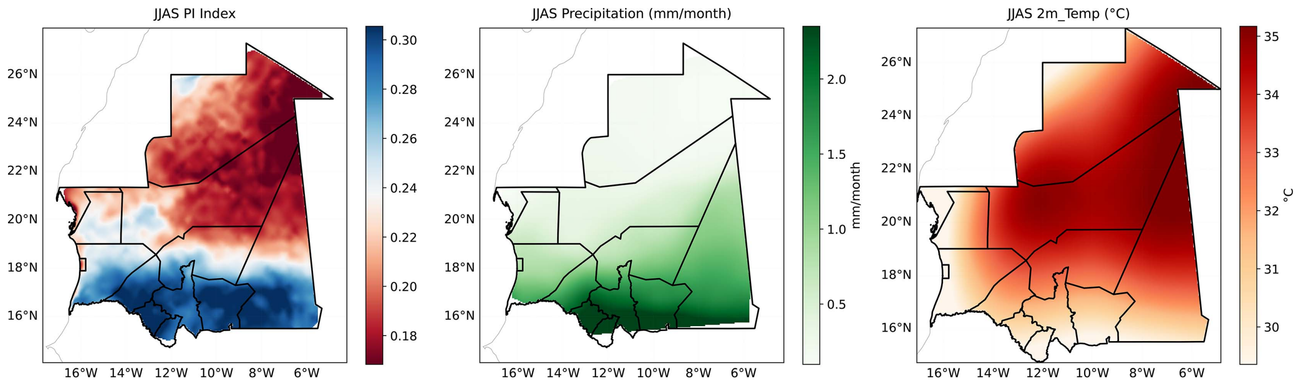

Figure 2. Spatial distribution of JJAS (June-September) climatology over Mauritania for the period 1979-2025 showing (a) Probability Index (PI), (b) precipitation (mm), and (c) 2m temperature (T2m ˚C). The results highlight a pronounced meridional gradient across the country.

Mann-Kendall trend analysis reveals distinct and divergent long-term trajectories for the three variables (**Figure 3**). The PI shows a statistically significant decreasing trend (Sen's slope: $-0.002729\ yr^{-1}$), corresponding to a cumulative decrease of approximately 0.18 over the 47-year study period. This systematic decline in PI indicates an intensification of compound dry-hot events that has progressed throughout the satellite era. Paradoxically, precipitation simultaneously shows a highly significant increasing trend (Sen's slope: $+0.0005\ mm\cdot yr^{-1}$), consistent with the well-documented Sahelian rainfall recovery and corresponding to an estimated gain of approximately 26 mm over the study period roughly 50% of the climatological seasonal mean. 2m temperature shows a positive but statistically non-significant trend ($p = +0.0269$), suggesting a weak warming tendency that does not reach conventional significance thresholds during JJAS, potentially because monsoon-associated cloud cover and evapotranspiration dampen the warming signal in wet season temperatures relative to the dry season.

The co-existence of increasing precipitation, stable 2 m temperatures, and declining PI values represents a paradoxical hydroclimatic trend: despite wetter conditions, compound dry-hot extremes have intensified. This likely reflects several interacting processes. First, the increase in precipitation may manifest as more intense but less frequent events rather than sustained increases in soil moisture, limiting evaporative cooling between episodes. Second, rising background temperatures from global warming may be counteracting the potential cooling effect of increased rainfall. Third, changes in cloud radiative properties and land surface feedbacks may modify the regional energy balance in ways not fully captured by the mean precipitation metric. This 'wetting without cooling' paradox has critical implications for climate risk assessment in the Sahel, demonstrating that precipitation recovery alone does not guarantee reduced compound climate risk.

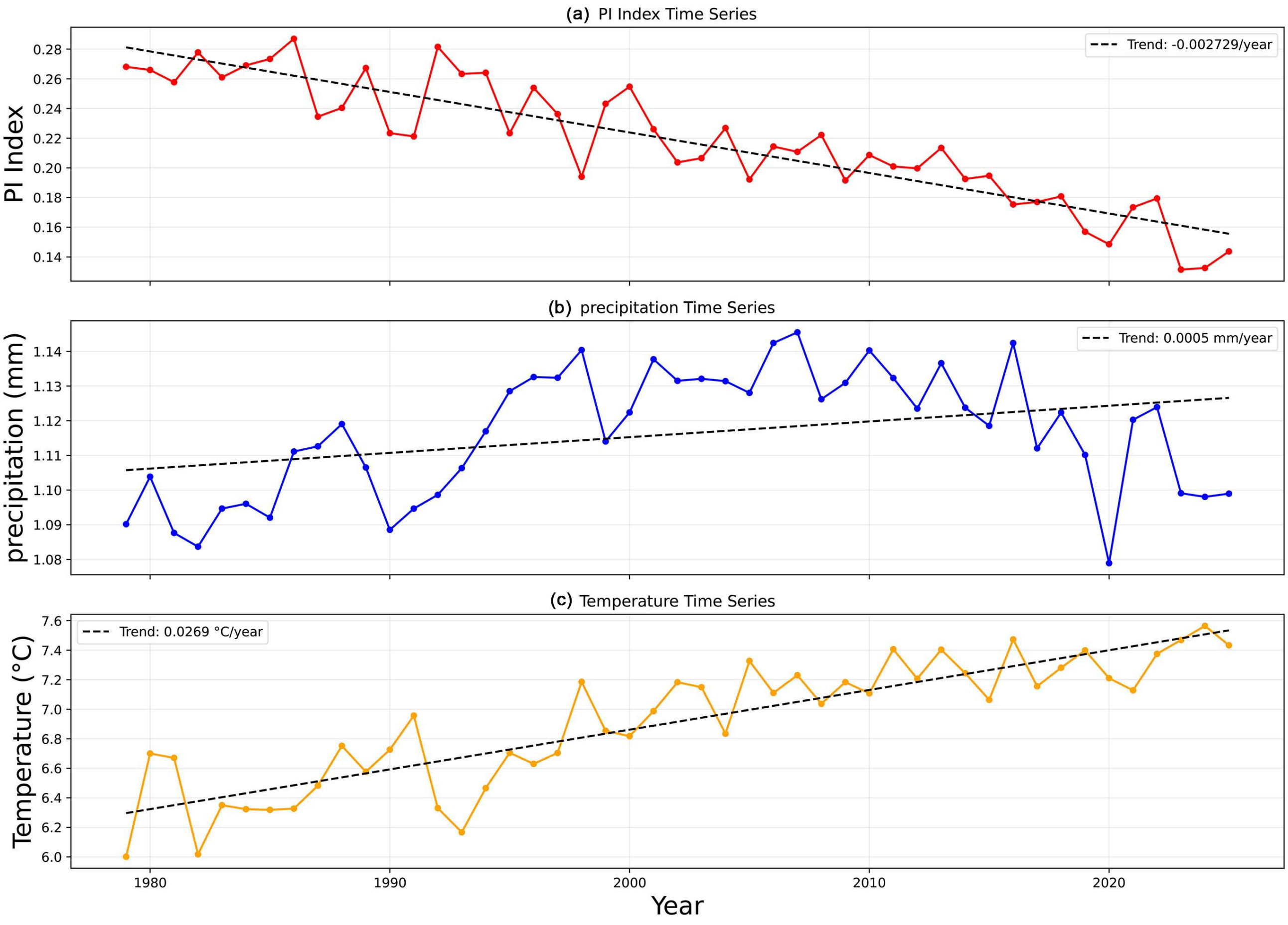

Figure 3. Time series of JJAS (June-September) (a) Probability Index (PI), (b) precipitation, and (c) 2 m temperature over Mauritania (1979-2025).

3.2. Dominant EOF Modes of Compound Dry-Hot Events

EOF analysis of the detrended JJAS PI field identifies two dominant, well-separated modes explaining approximately 69% of total interannual variance (Figure 4). The first mode (EOF1, 51.29%) exhibits a spatially coherent pattern with nearly uniform negative loadings across all of Mauritania (Figure 4(a)). Under the sign convention adopted in this study, negative loadings indicate that positive PC1 corresponds to intensified compound dry-hot conditions (lower PI values) across the entire country. Thus, positive PC1 drives country-wide intensification of compound extremes through concurrent basin-wide warming and precipitation deficits, while negative PC1 corresponds to relatively wetter and cooler conditions with suppressed compound dry-hot events. The PC1 time series (Figure 4(b)) shows pronounced interannual variability with a statistically significant upward trend, indicating that the large-scale spatially coherent mode of compound dry-hot conditions has intensified over time, which is consistent with the observed decreasing trend in PI (Figure 3(a)).

The second mode (EOF2, 16.51%) reveals a pronounced north-south dipole pattern with positive loadings over northern Mauritania and negative loadings over the south (Figure 4(c)). Under our sign convention, positive PC2 corresponds to a pattern where compound dry-hot events intensify in the south (negative loadings) while being simultaneously suppressed in the north (positive loadings). During negative PC2 phases, the opposite occurs: compound events intensify in the north and are suppressed in the south. Regression of 2 m temperature and precipitation onto the detrended PCs confirms this physical interpretation: positive PC2 corresponds to warming and reduced precipitation in the south with opposite (cooler/wetter) conditions in the north. The PC2 time series (Figure 4(d)) shows a modest downward trend, suggesting a gradual change in the dipole pattern over the study period. The north-south dipole structure of EOF2 implies the existence of regionally differentiated atmospheric circulation mechanisms that produce opposing impacts between the Sahelian south and the Saharan north.

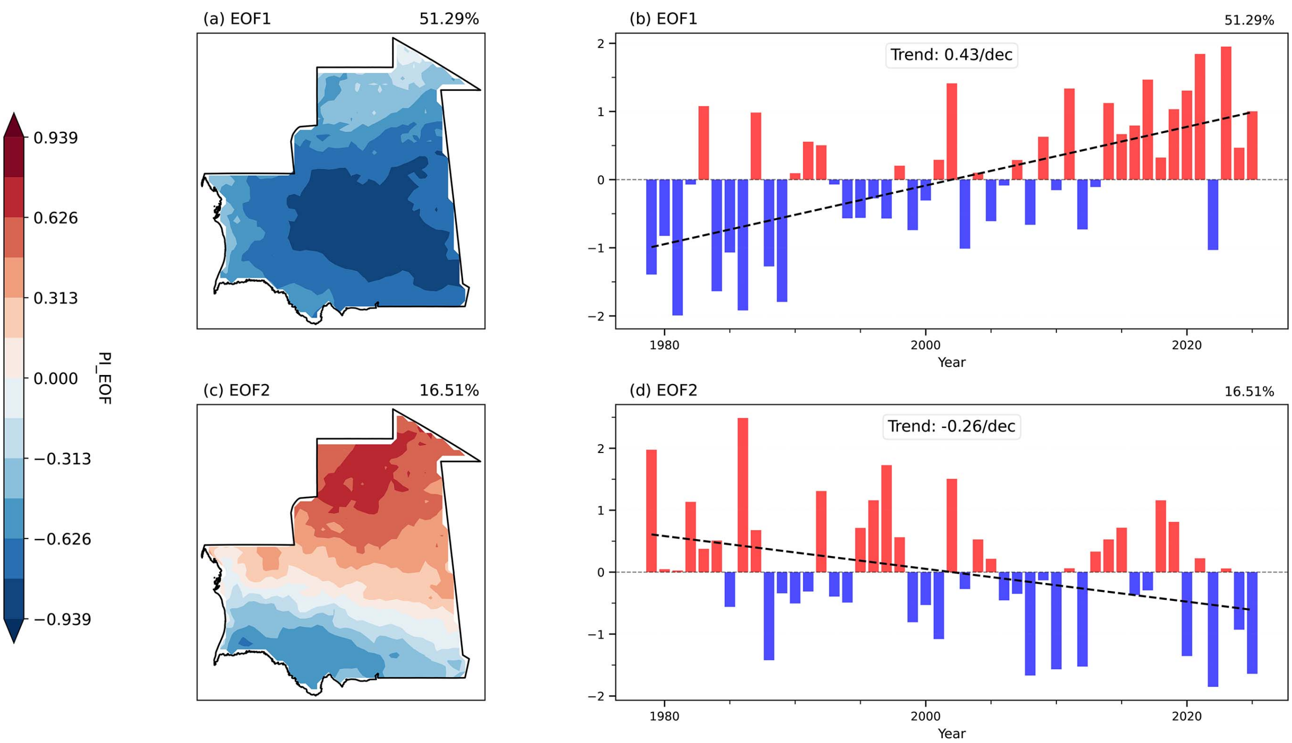

Figure 4. EOF analysis of the Summer (JJAS) Probability Index (PI) in Mauritania from 1979 to 2025: (a), (c) spatial patterns of the first two EOF modes (EOF1 and EOF2); (b), (d) the corresponding principal component time series (PC1 and PC2).

3.3. Atmospheric Circulation Anomalies

Regression analysis of horizontal wind fields onto the detrended PCs reveals fundamentally distinct circulation structures at both lower (700 hPa) and upper (300 hPa) tropospheric levels (Figure 5, Figure 6). PC1 is associated with a deep, vertically coherent anticyclonic circulation centered over Mauritania, exhibiting an equivalent barotropic structure extending consistently from the lower to the upper troposphere. This coherent anticyclonic anomaly implies large-scale dynamical control as the primary driver of the spatially uniform mode of compound dry-hot risk. The 500 hPa geopotential height field regressed onto PC1 shows a broad, statistically significant positive anomaly (anomalous ridge) centered over Mauritania and extending across much of the West African Sahel, confirming upper-level anticyclonic conditions favorable for subsidence. Vertical wind field analysis confirms robust, vertically coherent subsidence below 500 hPa over 15˚N - 22˚N, significant at the 90% confidence level. This subsidence suppresses convective activity, reduces cloud cover, and drives adiabatic near-surface warming establishing a positive feedback loop that amplifies compound dry-hot conditions across the entire country.

PC2 generates a contrasting meridional dipole circulation: anomalous cyclonic circulation over northern Mauritania and anticyclonic circulation over the southern portion, both also exhibiting equivalent barotropic vertical structure from 850 to 200 hPa. The cyclonic anomaly in the north promotes convergence, cloudiness,

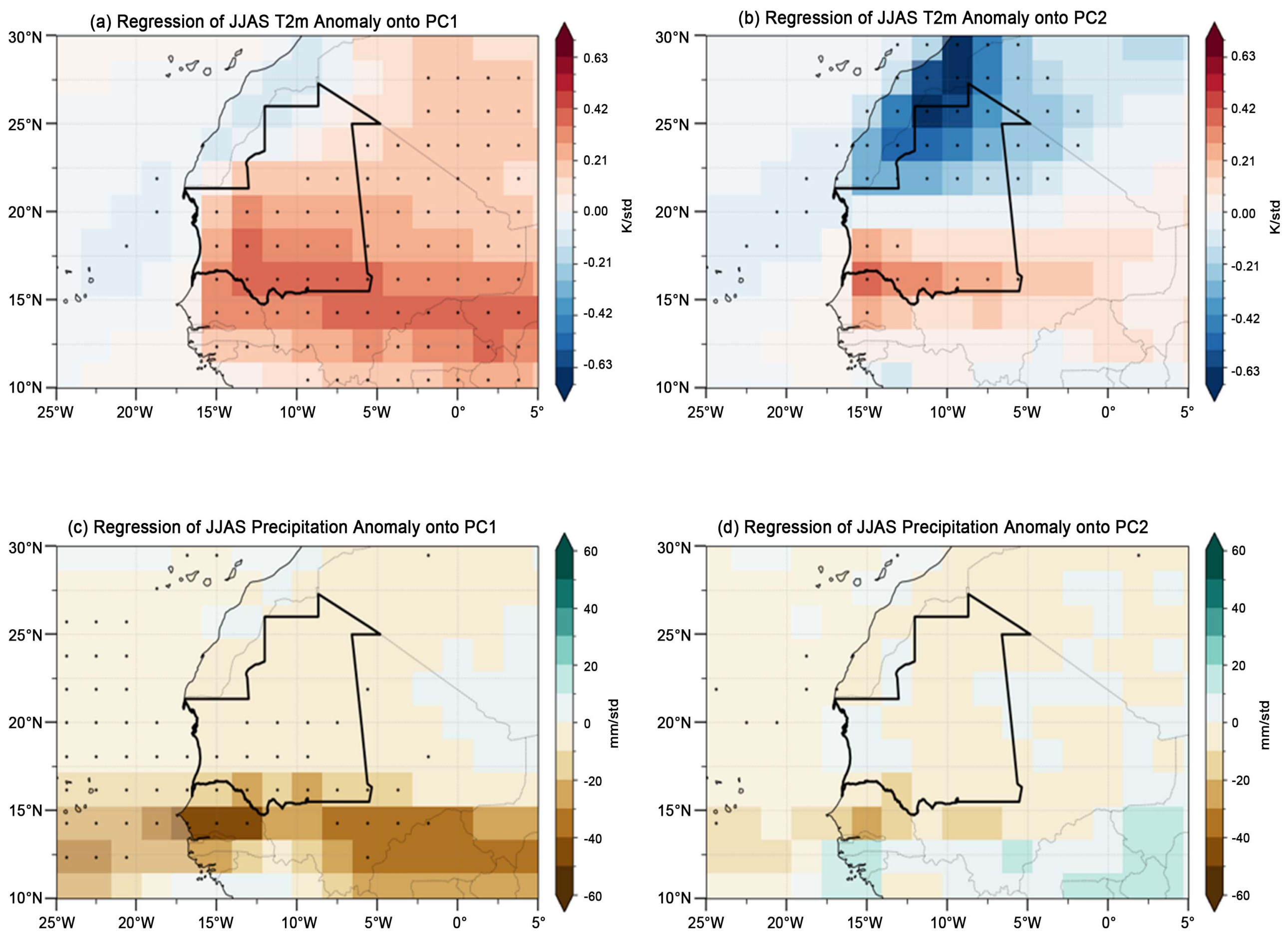

Figure 5. Regression of (a) JJAS precipitation and (c) 2 m temperature fields onto the detrended PC1; (b) and (d) are the same as (a) and (c) but for the detrended PC2.

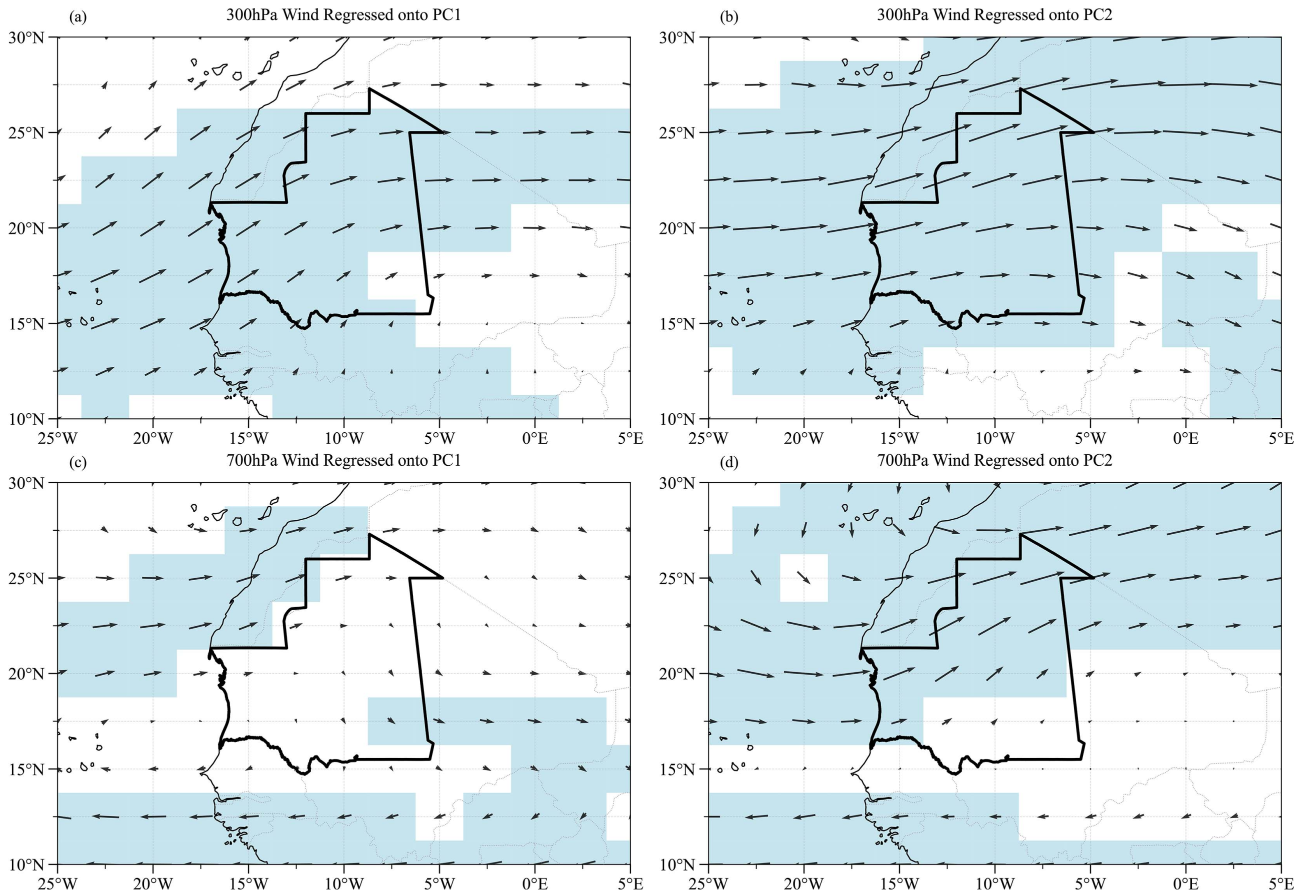

Figure 6. Regression of (a), (b) 300 hPa and (c), (d) 700 hPa horizontal wind fields onto (a), (c) the detrended PC1 and (b), (d) the detrended PC2. Areas significant at the 90% confidence level are indicated by blue shading.

and rainfall enhancement, while the anticyclonic anomaly in the south drives subsidence, clear skies, and warming. This opposing circulation configuration physically explains the north-south dipole of EOF2 and suggests that PC2 modulates compound dry-hot events primarily through regional atmospheric dynamics rather than deep coherent subsidence. The weaker and more localized vertical motion signal for PC2 is consistent with a more regionalized forcing mechanism that differentially affects the northern and southern climatic zones of Mauritania.

3.4. Statistical Linkage between ENSO Diversity and PI Modes

This anomalous descent, significant at the 90% confidence level, is consistent with the upper-level anticyclonic ridge observed in the 500 hPa geopotential height field (Figure 7(a)) and the deep anticyclonic circulation identified in the horizontal wind analysis (Figure 6(a), Figure 6(c)). Together, these features depict a coupled dynamical response to PC1: an upper-level ridge promoting large-scale subsidence, which suppresses convective activity and reinforces anticyclonic conditions throughout the tropospheric column. The subsidence is most pronounced in the mid-to-lower troposphere, suggesting a mechanism that inhibits vertical motion and reduces the potential for deep convection, thereby exerting a drying influence on the region.

In contrast, the regression onto PC2 exhibits a more complex vertical circulation pattern (**Figure 7(b)**). A weak and largely insignificant ascent is suggested over northern Mauritania, while a shallow layer of subsidence appears over the central and southern portions of the country, though these features are less vertically coherent and exhibit limited statistical significance.

Correlations between the PCs and preceding spring (MAM) tropical Pacific SST anomalies reveal distinct and physically interpretable SST patterns for each mode (**Figure 8**). PC1 correlates with a zonal dipole SST structure with significant positive correlations (r > 0.6) extending across the central-eastern equatorial Pacific, accompanied by negative correlations over the western Pacific, characteristic of canonical EP ENSO. PC2 correlates with a tripolar SST pattern with significant positive correlations centered near the dateline, with negative correlations on both the eastern and western flanks, characteristic of CP ENSO (El Niño Modoki). These contrasting SST correlation structures confirm that the two dominant PI modes are driven by physically distinct ENSO flavors, with the EP type governing basin-wide compound dry-hot event variability and the CP type governing the meridional dipole pattern.

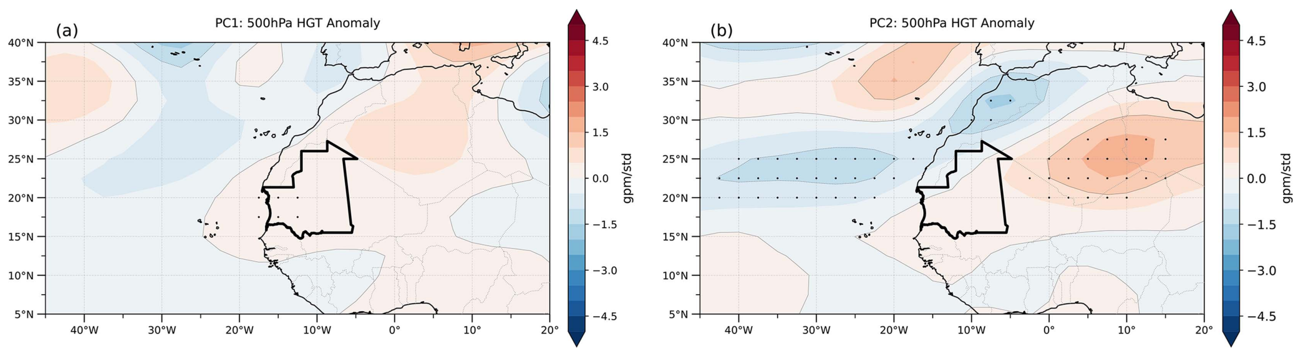

Figure 7. 500-hPa geopotential height anomalies regressed onto the detrended (a) PC1 and (b) PC2. Note that the zonal mean has been removed from the height field.

Scatter plot and correlation analysis using the Ren and Jin (Ren & Jin, 2011) orthogonal ENSO indices quantify these relationships (**Figure 8**). PC1 shows a highly significant positive correlation with the EP index (r = 0.55, $p < 0.001$) and negligible correlation with the CP index (r = 0.19, $p = 0.211$). Conversely, PC2 shows a significant positive correlation with the CP index (r = 0.38, $p = 0.0082$) and negligible correlation with the EP index (r = 0.12, $p = 0.438$). These near-zero cross-correlations confirm the independence of the two ENSO teleconnection pathways and validate the utility of the orthogonal indices for disentangling distinct ENSO impacts. EP ENSO selectively governs the spatially coherent country-wide mode, while CP ENSO selectively governs the meridional dipole mode. This selective modulation has important forecasting implications: EP ENSO-based seasonal predictions can be applied uniformly across Mauritania, while CP ENSO-based predictions require regional differentiation between northern and southern zones. The temporal co-variability reinforces these linkages (Figure 9). Major El Niño events, including the strong EP events of 1982-83, 1991-92, 1997-98, and 2015-16, correspond to notable positive PC1 excursions, reflecting intensified country-wide compound dry-hot conditions during these years (consistent with the positive correlation between PC1 and the EP index). The PC2 time series co-varies with the CP ENSO index, with CP El Niño events corresponding to positive PC2 phases, enhanced compound dry-hot conditions in the south, and suppressed conditions in the north. The alignment in phase between the PC and ENSO time series further confirms the robustness of the selective teleconnection pathways identified here.

3.5. Physical Mechanisms of EP and CP ENSO Impacts

Regression of JJAS PI, temperature, precipitation, specific humidity, OLR, geopotential height, stream function, and velocity potential onto the MAM ENSO

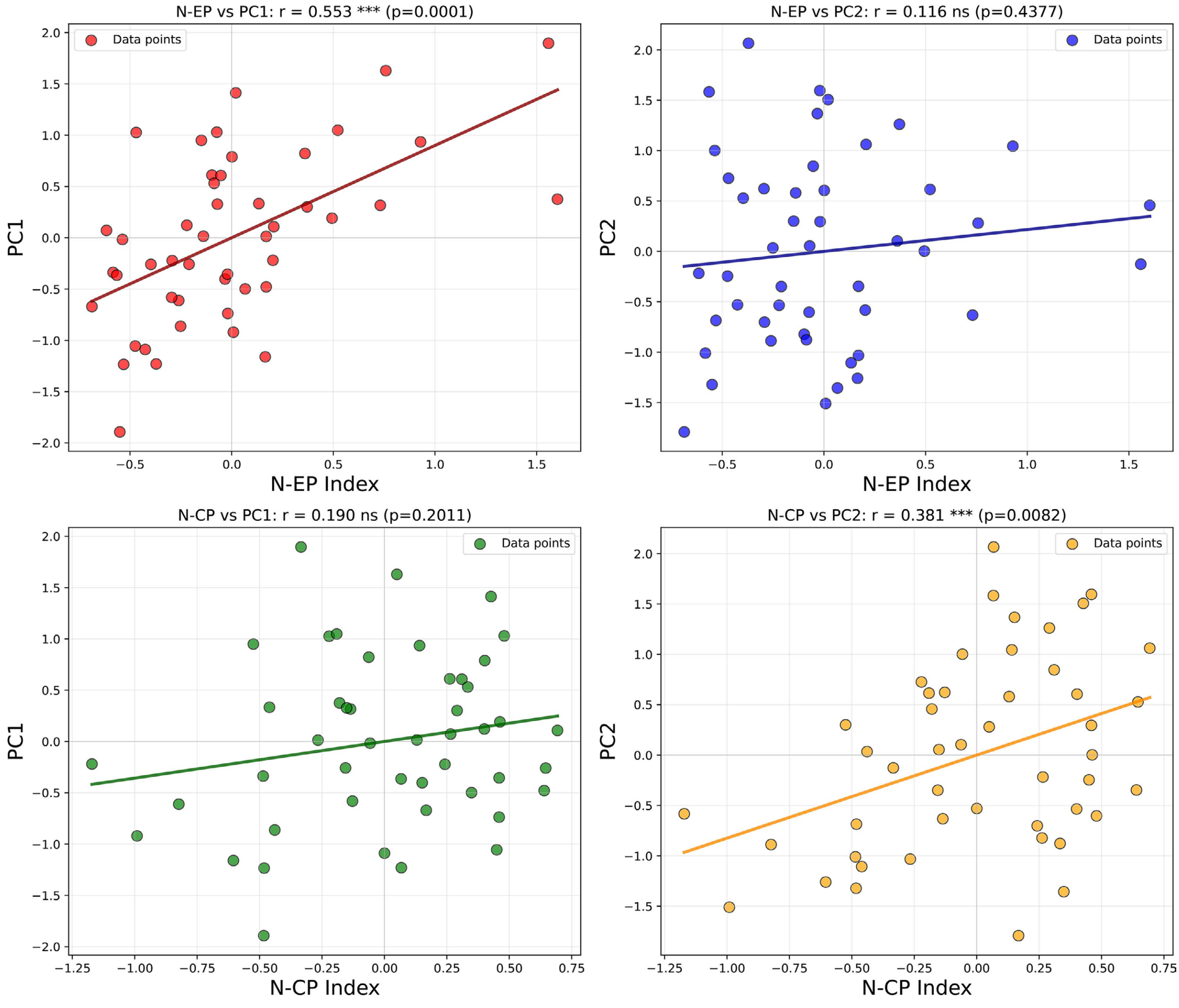

Figure 8. Scatter plots of PC1 and PC2 of PI in Mauritania against the MAM EP and CP Nino indices.

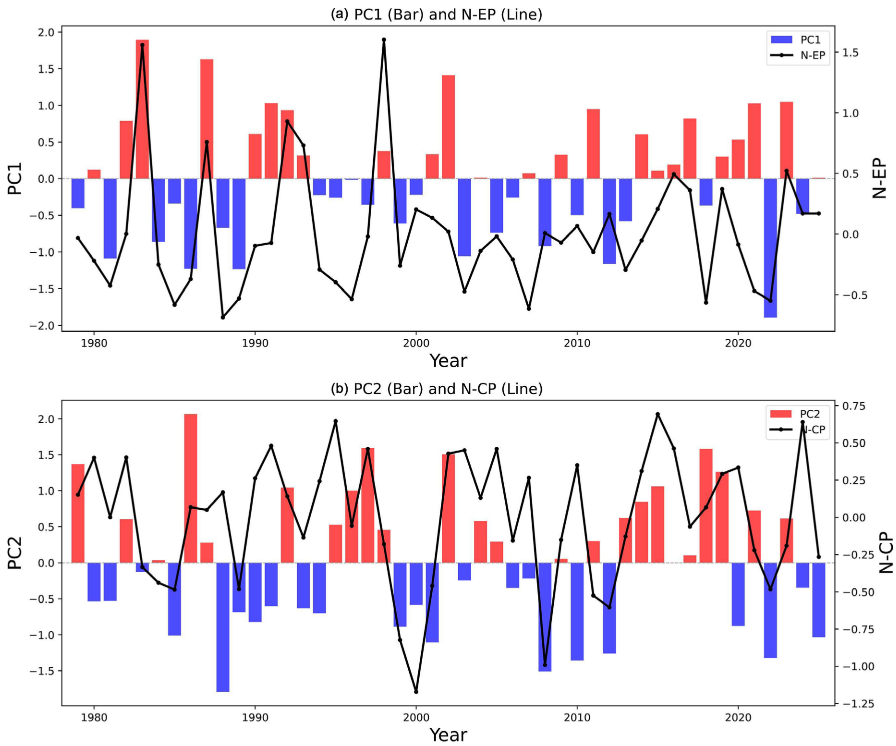

Figure 9. Time series of (a) PC1 (bars) and the EP index (line), and (b) PC2 (bars) and the CP index (line).

indices reveals contrasting physical mechanisms for the two ENSO types (Figures 10-13). During EP-type El Niño events, compound hot-dry events increase significantly across the entire country, accompanied by widespread positive temperature anomalies and negative precipitation anomalies particularly in the southern Sahelian zone. Vertically integrated specific humidity exhibits negative anomalies over most of Mauritania, while OLR shows positive anomalies, confirming suppressed convection and reduced cloudiness. Positive geopotential height anomalies dominate at all tropospheric levels (200, 500, and 850 hPa) over the West African region, indicating large-scale high-pressure conditions favorable for subsidence. Stream function diagnostics confirm anomalous upper-level convergence and lower-level divergence over the region, enhancing anomalous descent. This subsidence drives adiabatic warming, suppresses moist convection, reduces cloud formation, and increases surface shortwave radiation, establishing positive thermodynamic feedback that amplifies compound dry-hot event risk basin-wide.

The underlying dynamical mechanism operates through Walker circulation adjustments: anomalous warming in the eastern equatorial Pacific intensifies convection there while inducing compensating large-scale subsidence over the Atlantic sector and West Africa (Giannini et al., 2003; Janicot et al., 1996; Bjerknes, 1969). This anomalous subsidence weakens the continental convergence associated with the WAM, reduces moisture transport into the Sahel, suppresses deep convection, and reduces monsoon rainfall, while simultaneously increasing near-surface temperatures through adiabatic warming the classic Bjerknes feedback mechanism operating in reverse over West Africa (Bjerknes, 1969). The persistent, deep vertical subsidence associated with EP ENSO is the key dynamical driver of compound dry-hot event risk across all of Mauritania during these events.

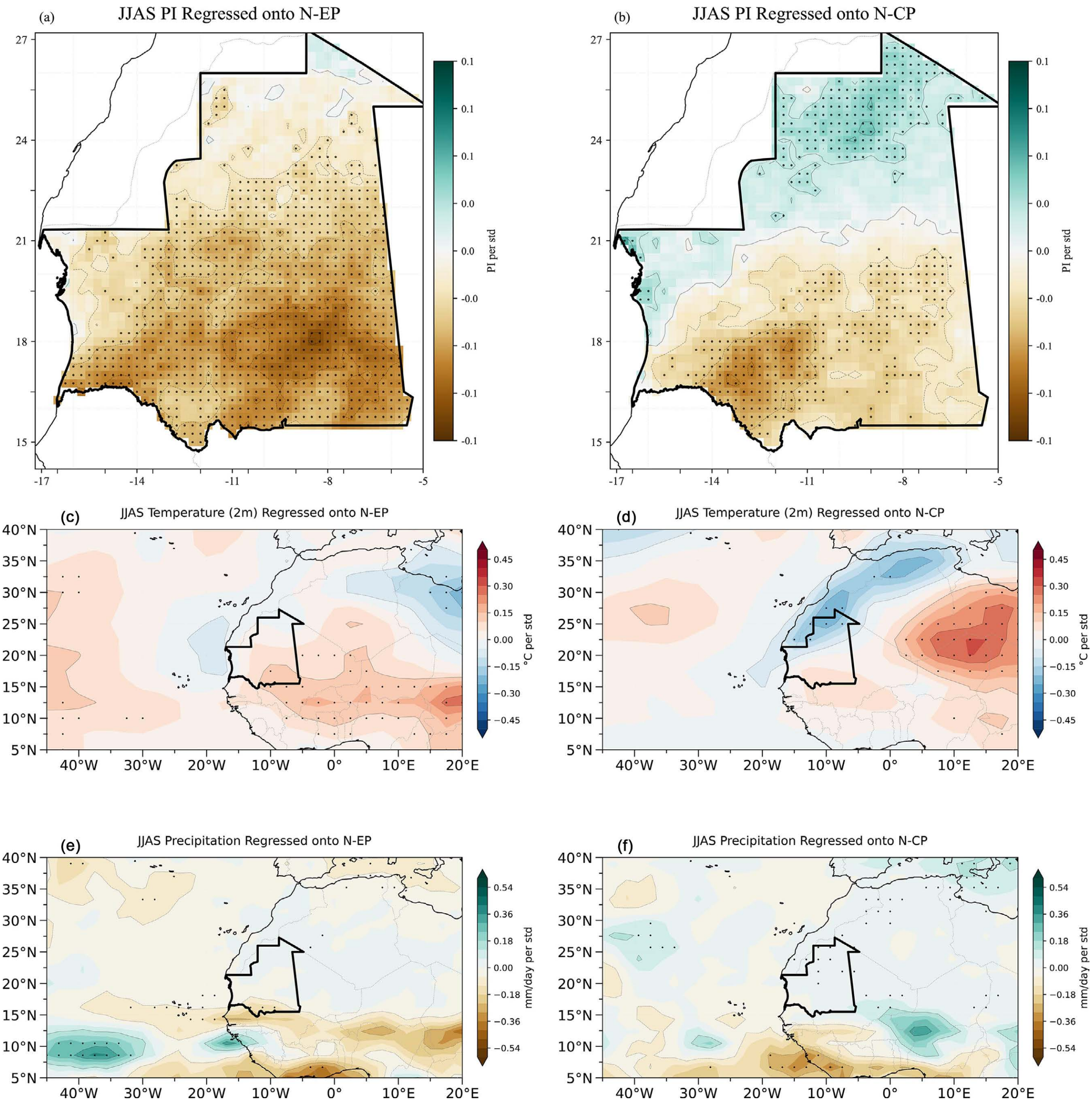

Figure 10. Regression of summer (JJAS) PI (a), (b), 2 m air temperature (c), (d), and precipitation (e), (f) fields onto the spring (MAM) EP and CP ENSO indices for the period 1979-2025. Stippled areas indicate regions that are significant at the 90% confidence level. The long-term linear trend has been removed from all datasets.

CP-type El Niño produces a strikingly different pattern. Compound hot-dry events display a pronounced north-south contrast, increasing significantly in the south while decreasing in the north. Temperature exhibits significant positive anomalies in the southeast and negative anomalies in the northwest, while precipitation shows significant positive anomalies in the north. Geopotential height analysis reveals significant positive anomalies at all tropospheric levels over southern Mauritania but negative anomalies over the northern region (Figure 11). CP-type El Niño favors anomalous anticyclonic circulation in the upper troposphere over northern Mauritania that promotes upward motion, enhanced moisture transport, and precipitation conditions unfavorable for compound dry-hot events in the north (Figure 12, Figure 13). Over southern Mauritania, the subsidence response promotes warming and dry conditions, favoring compound event development.

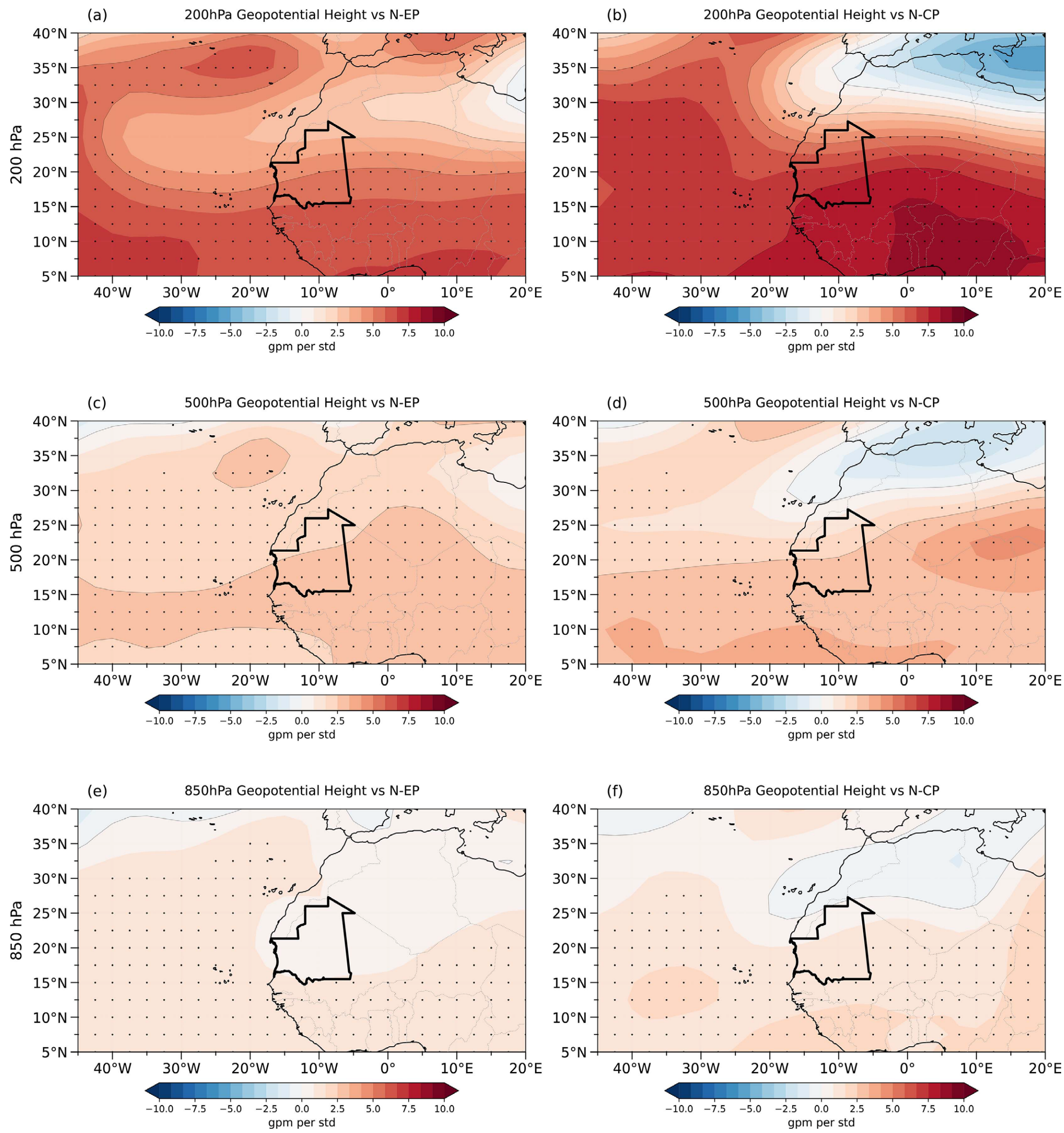

Figure 11. Regression of summer (JJAS) geopotential height fields at 200 hPa (a), (b), 500 hPa (c), (d), and 850 hPa (e), (f) onto the spring (MAM) EP and CP ENSO indices. Stippled areas indicate regions significant at the 90% confidence level.

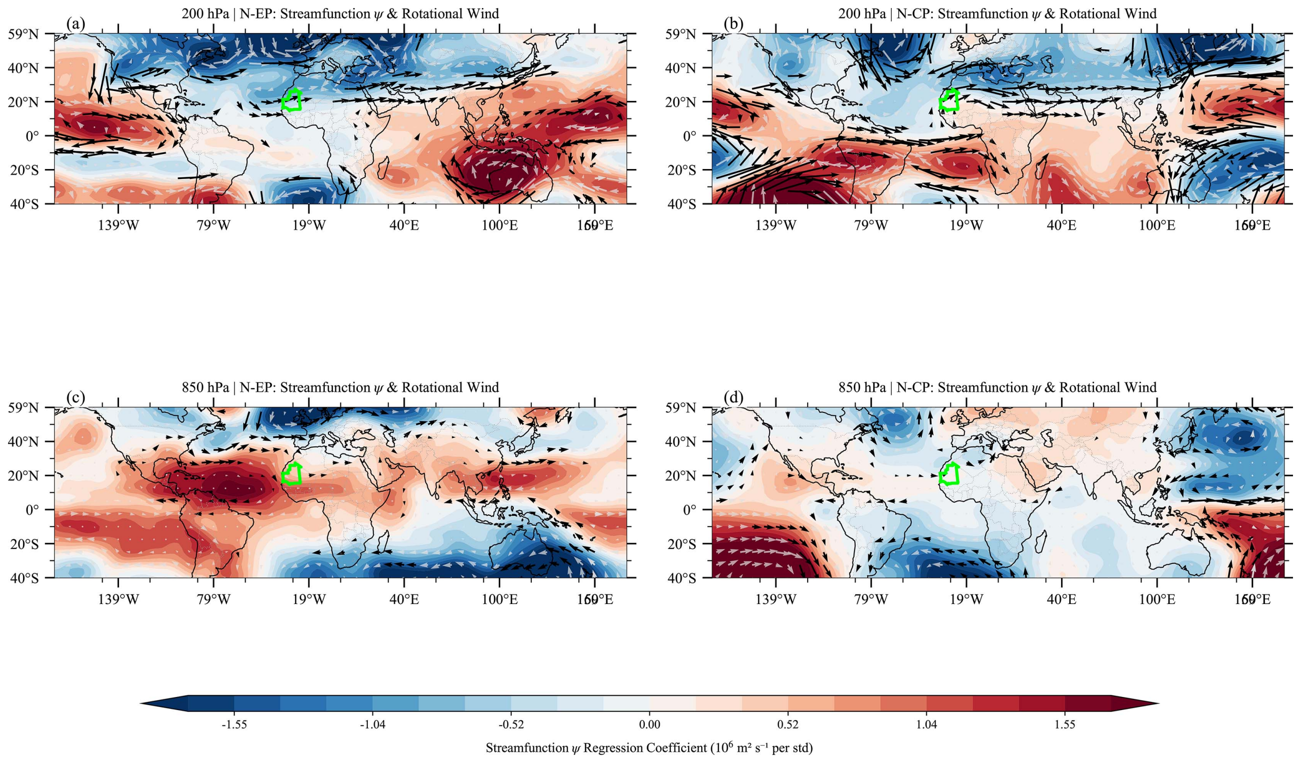

Figure 12. Summer (JJAS) stream function (shading) and rotational wind (vectors) at 200 hPa (a), (c) and 850 hPa (b), (d) regressed onto the spring (MAM) EP and CP ENSO indices. Black vectors indicate rotational wind anomalies that are significant at the 90% confidence level.

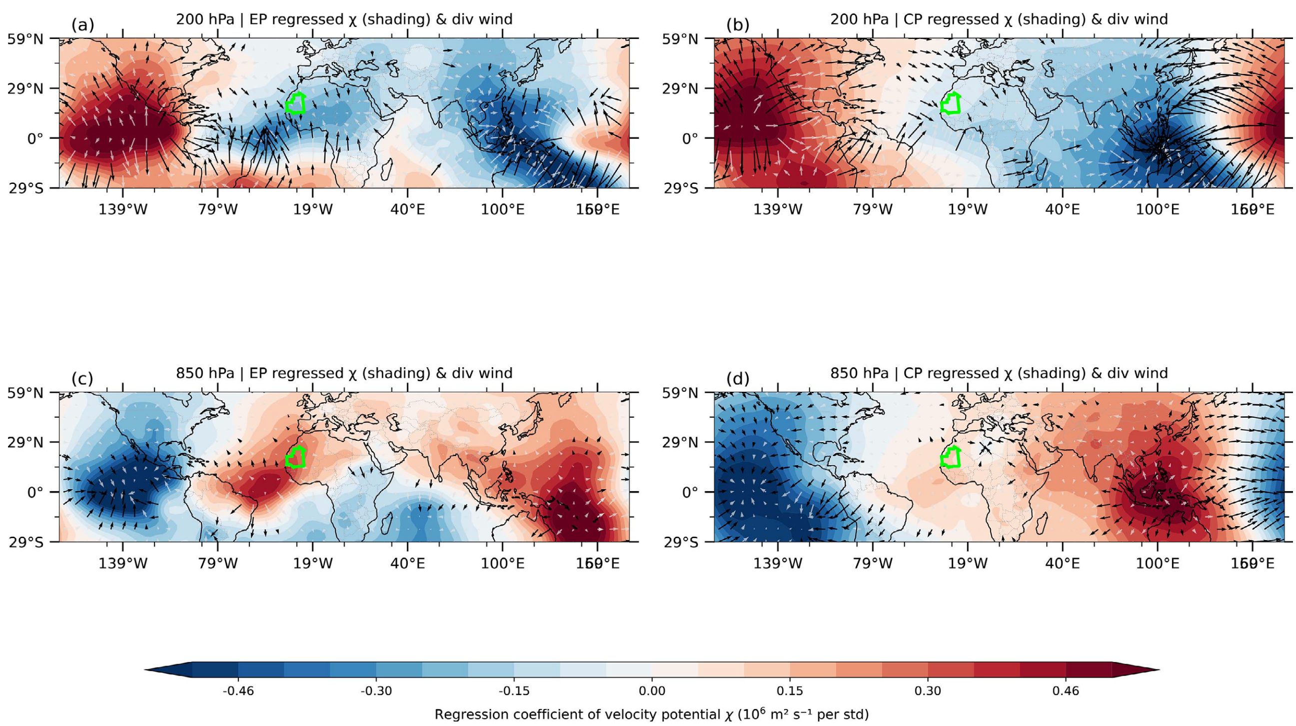

Figure 13. Summer (JJAS) velocity potential (shading) and divergent wind (vectors) at 200 hPa (a), (c) and 850 hPa (b), (d) regressed onto the spring (MAM) EP and CP ENSO indices. Black vectors indicate divergent wind anomalies that are significant at the 90% confidence.

The mechanistic pathway for CP ENSO involves the westward shift of SST anomaly maximum toward the central Pacific, which alters the Walker circulation structure and generates a distinct Rossby wave response with different phase alignment compared to EP ENSO (Ashok et al., 2007; Preethi et al., 2015; Kao & Yu, 2009). Due to this westward shift, the descending branch of the CP ENSO-perturbed Walker circulation over Africa is displaced meridionally relative to the EP case, producing anomalous subsidence over the southern Sahelian zone while the northern zone is influenced by the anomalous ascending branch or by extratropical wave dynamics. This meridional contrast in vertical motion ultimately drives the north-south dipole in compound dry-hot event risk that characterizes EOF2. The physical coherence between the statistical linkages identified in Section 3.4 and the dynamical mechanisms presented here provides strong evidence for the causal relationships governing ENSO-compound dry-hot event interactions over Mauritania.

To summarize the comparative mechanisms: EP El Niño warming in the eastern Pacific enhances convective activity there, driving compensating large-scale subsidence over West Africa through Walker circulation adjustments, leading to uniform compound dry-hot event intensification across all of Mauritania. CP El Niño warming near the dateline perturbs the Walker circulation more weakly and generates a different meridional distribution of vertical motion anomalies over the West African sector, producing subsidence in the Sahelian south while the Saharan north experiences anomalous ascent creating the north-south dipole that distinguishes the CP ENSO response from the EP type. These contrasting mechanisms have direct practical implications: while the occurrence of a strong EP El Niño event in the preceding spring provides a reliable signal of elevated compound dry-hot event risk across all of Mauritania in the following summer, a CP El Niño event calls for a spatially nuanced forecast with elevated risk in the south and potentially reduced risk in the north. Conversely, CP La Niña events would be expected to reduce compound event risk in the south while potentially increasing it in the north, a differentiated regional forecast that would not be captured by standard ENSO-phase monitoring alone. The results of this study thus advance the physical understanding of how ENSO diversity shapes compound climate extremes in the Sahel and provide the scientific foundation for regionally differentiated seasonal climate forecasts in Mauritania.

4. Conclusion and Discussion

4.1. Conclusion

This study provides the first comprehensive assessment of compound dry-hot event variability over Mauritania (1979-2025) using a multivariate Probability Index framework, systematically linking dominant modes of compound dry-hot event variability to distinct ENSO types through physically coherent atmospheric circulation diagnostics. Four major conclusions emerge from the analysis. **First, a paradoxical hydroclimatic trend.** Over the 47-year study period, JJAS precipitation has increased significantly (+0.049 mm·yr^{-1}, $p = 0.000$) consistent with the Sahelian rainfall recovery, yet the Probability Index has simultaneously declined significantly −0.0036 yr^{-1}, $p < 0.001$), indicating an intensification of compound dry-hot events. 2 m temperature shows no statistically significant trend (p = 0.122). This paradoxical co-existence of increased rainfall and more frequent compound dry-hot extremes challenges the conventional expectation that wetter conditions reduce compound dry-hot event risk. It points to complex thermodynamic-dynamic interactions between global warming, changing rainfall characteristics, and land-atmosphere feedbacks that cannot be captured by single-variable drought indices. The finding has critical policy relevance: Mauritania's observed rainfall recovery since the 1980s has not reduced, and may even coincide with, heightened compound climate risk fundamentally altering the calculus for climate adaptation planning. **Second, two dominant modes of compound event variability.** EOF analysis identifies two well-separated leading modes accounting for 69% of total interannual variance. EOF1 (51.29%) captures spatially coherent country-wide variability driven by concurrent basin-wide temperature and precipitation anomalies, associated with deep vertically coherent tropospheric anticyclonic circulation and subsidence over the entire country. EOF2 (16.51%) captures a north-south dipole driven by opposing circulation anomalies between the Saharan north and the Sahelian south, with distinct implications for regional compound dry-hot event risk that vary latitudinally across the country. **Third, selective modulation by ENSO types.** Correlation analysis establishes a clear, statistically robust, and selective linkage: EP ENSO governs EOF1 (PC1–N-EP: r = 0.55, $p < 0.001$; PC1–N-CP: r = 0.19, ns) while CP ENSO governs EOF2 (PC2–N-CP: r = 0.38, $p < 0.01$; PC2–N-EP: r = 0.12, ns). The near-zero cross-correlations confirm orthogonal teleconnection pathways. This implies EP ENSO-based seasonal forecasts can be applied uniformly across Mauritania, while CP ENSO-based forecasts must be spatially differentiated to account for the opposing compound event responses in the north versus the south. **Fourth, distinct physical mechanisms.** EP El Niño induces country-wide compound event risk through Walker circulation-driven large-scale subsidence that suppresses convection, reduces atmospheric moisture, increases surface temperature via adiabatic warming, reduces cloud cover to enhance surface shortwave radiation, and establishes a positive thermodynamic feedback loop. CP El Niño generates a meridionally asymmetric response through its distinct SST structure and Walker circulation perturbation: anomalous subsidence and warming in the south promoting compound dry-hot events, anomalous ascent and moisture enhancement in the north suppressing them, producing the observed dipole pattern consistent with EOF2. The physical mechanisms are thus qualitatively different in character, amplitude, and spatial organization for the two ENSO types.

4.2. Discussion

Operational seasonal forecasting. National meteorological agencies in Mauritania and the broader Sahel region should incorporate ENSO-type classification explicitly distinguishing EP from CP ENSO into seasonal forecast frameworks rather than relying solely on ENSO phase. The identification of statistically significant precursor spring (MAM) ENSO signals for summer compound event risk provides a physical basis for extending forecast leads times to 2 - 3 months. Given the contrasting CP ENSO response between northern and southern Mauritania, forecast products must deliver spatially disaggregated risk estimates. Integration of the Probability Index into operational forecast systems would provide a more comprehensive risk metric than traditional single-variable precipitation forecasts. Regional early warning systems should incorporate compound dry-hot event probability metrics based on ENSO diversity to enable timely humanitarian response and agricultural planning.

Climate risk assessment and adaptation. Risk assessments must move beyond single-variable drought indices toward multivariate compound dry-hot event frameworks. The paradoxical intensification of compound dry-hot events alongside precipitation recovery demonstrates that 'wetter does not mean safer' in contemporary Mauritania. This challenges development planning assumptions and underscores the need for adaptation strategies that simultaneously address both moisture deficits and thermal extremes. Policy interventions should prioritize climate-resilient crop varieties tolerant to both heat stress and moisture variability, investment in water storage infrastructure to buffer the impacts of intense but infrequent rainfall events, and strengthening of heat-health early warning systems for vulnerable populations.

Future research priorities. Several important directions are identified. A limitation of this study is the inability to perform a formal quantitative attribution of the PI trend into temperature versus precipitation contributions. Furthermore, future studies should validate the identified teleconnection pathways across multiple modern reanalysis products (ERA5, JRA-55) to assess the robustness of results to reanalysis uncertainty. Moreover, the roles of other large-scale forcings including the Atlantic Niño, Atlantic Meridional Mode, Indian Ocean Dipole, and Mediterranean SST in modulating compound dry-hot events and potentially interacting with ENSO teleconnections warrant systematic investigation. Third, attribution studies using detection-attribution methodologies are needed to determine the extent to which anthropogenic climate change is modifying the ENSO-compound dry-hot event relationship, particularly given projections of increased CP ENSO frequency under future warming (Cai et al., 2014). Fourth, process-based studies should examine the roles of the African Easterly Jet, Tropical Easterly Jet, and Saharan Heat Low in mediating the CP ENSO dipole response over Mauritania. Fifth, machine-learning prediction models integrating multiple precursor climate indices with spatially disaggregated risk estimates would substantially advance operational seasonal forecasting capabilities to protect Mauritania's vulnerable population from compound climate extremes.

Acknowledgments

The authors gratefully acknowledge the National Centers for Environmental Prediction-National Center for Atmospheric Research (NCEP-NCAR) for providing the reanalysis datasets, and the National Oceanic and Atmospheric Administration (NOAA) for the ERSSTv5 sea surface temperature dataset accessed via the IRI/LDEO Climate Data Library. This research was conducted at the School of Atmospheric Sciences, Nanjing University of Information Science and Technology (NUIST), Nanjing, China.

Funding

This research is jointly supported by the Independent Research Program of the National Key Laboratory of Climate System Prediction and Climate Change Response (CPRM-2025-NUIST-012).

Conflicts of Interest

The authors declare no conflicts of interest regarding the publication of this paper.

References

AghaKouchak, A., Cheng, L., Mazdiyasni, O., & Farahmand, A. (2014). Global Warming and Changes in Risk of Concurrent Climate Extremes: Insights from the 2014 California Drought. *Geophysical Research Letters, 41,* 8847-8852. https://doi.org/10.1002/2014gl062308

Ashok, K., Behera, S. K., Rao, S. A., Weng, H., & Yamagata, T. (2007). El Niño Modoki and Its Possible Teleconnection. *Journal of Geophysical Research: Oceans, 112,* C11007. https://doi.org/10.1029/2006jc003798

Bjerknes, J. (1969). Atmospheric Teleconnections from the Equatorial Pacific. *Monthly Weather Review, 97,* 163-172. https://doi.org/10.1175/1520-0493(1969)097<0163:atftep>2.3.co;2

Cai, W., Borlace, S., Lengaigne, M., van Rensch, P., Collins, M., Vecchi, G. et al. (2014). Increasing Frequency of Extreme El Niño Events Due to Greenhouse Warming. *Nature Climate Change, 4,* 111-116. https://doi.org/10.1038/nclimate2100

Chow, V. T. (1964). *Handbook of Applied Hydrology.* McGraw-Hill.

Diffenbaugh, N. S., Singh, D., Mankin, J. S., Horton, D. E., Swain, D. L., Touma, D. et al. (2017). Quantifying the Influence of Global Warming on Unprecedented Extreme Climate Events. *Proceedings of the National Academy of Sciences of the United States of America, 114,* 4881-4886. https://doi.org/10.1073/pnas.1618082114

Giannini, A., Biasutti, M., & Verstraete, M. M. (2008). A Climate Model-Based Review of Drought in the Sahel: Desertification, the Re-Greening and Climate Change. *Global and Planetary Change, 64,* 119-128. https://doi.org/10.1016/j.gloplacha.2008.05.004

Giannini, A., Saravanan, R., & Chang, P. (2003). Oceanic Forcing of Sahel Rainfall on Interannual to Interdecadal Time Scales. *Science, 302,* 1027-1030. https://doi.org/10.1126/science.1089357

Hannachi, A., Jolliffe, I. T., & Stephenson, D. B. (2007). Empirical Orthogonal Functions and Related Techniques in Atmospheric Science: A Review. *International Journal of Climatology, 27,* 1119-1152. https://doi.org/10.1002/joc.1499

IPCC (2021). *Climate Change 2021: The Physical Science Basis. Contribution of Working Group I to the Sixth Assessment Report of the Intergovernmental Panel on Climate Change.* Cambridge University Press.

Janicot, S., Moron, V., & Fontaine, B. (1996). Sahel Droughts and Enso Dynamics. *Geophysical Research Letters, 23,* 515-518. https://doi.org/10.1029/96gl00246

Joly, M., & Voldoire, A. (2009). Influence of ENSO on the West African Monsoon: Temporal Aspects and Atmospheric Processes. *Journal of Climate, 22,* 3193-3210. https://doi.org/10.1175/2008jcli2450.1

Kalnay, E., Kanamitsu, M., Kistler, R., Collins, W., Deaven, D., Gandin, L. et al. (1996). The NCEP/NCAR 40-Year Reanalysis Project. *Bulletin of the American Meteorological Society, 77,* 437-471. https://doi.org/10.1175/1520-0477(1996)077<0437:tnyrp>2.0.co;2

Kao, H., & Yu, J. (2009). Contrasting Eastern-Pacific and Central-Pacific Types of Enso. *Journal of Climate, 22,* 615-632. https://doi.org/10.1175/2008jcli2309.1

Kug, J., Jin, F., & An, S. (2009). Two Types of El Niño Events: Cold Tongue El Niño and Warm Pool El Niño. *Journal of Climate, 22,* 1499-1515. https://doi.org/10.1175/2008jcli2624.1

Larkin, N. K., & Harrison, D. E. (2005). On the Definition of El Niño and Associated Seasonal Average U.S. Weather Anomalies. *Geophysical Research Letters, 32,* L13705. https://doi.org/10.1029/2005gl022738

Lee, T., & McPhaden, M. J. (2010). Increasing Intensity of El Niño in the Central-Equatorial Pacific. *Geophysical Research Letters, 37,* L14603. https://doi.org/10.1029/2010gl044007

Nicholson, S. (2005). On the Question of the "Recovery" of the Rains in the West African Sahel. *Journal of Arid Environments, 63,* 615-641. https://doi.org/10.1016/j.jaridenv.2005.03.004

Nicholson, S. E. (2013). The West African Sahel: A Review of Recent Studies on the Rainfall Regime and Its Interannual Variability. *ISRN Meteorology, 2013,* Article ID: 453521. https://doi.org/10.1155/2013/453521

Preethi, B., Sabin, T. P., Adedoyin, J. A., & Ashok, K. (2015). Impacts of the ENSO Modoki and Other Tropical Indo-Pacific Climate-Drivers on African Rainfall. *Scientific Reports, 5,* Article No. 16653. https://doi.org/10.1038/srep16653

Ren, H., & Jin, F. (2011). Niño Indices for Two Types of Enso. *Geophysical Research Letters, 38,* L04704. https://doi.org/10.1029/2010gl046031

Rowell, D. P. (2001). Teleconnections between the Tropical Pacific and the Sahel. *Quarterly Journal of the Royal Meteorological Society, 127,* 1683-1706. https://doi.org/10.1002/qj.49712757512

Salvadori, G., Durante, F., & De Michele, C. (2013). Multivariate Return Period Calculation via Survival Functions. *Water Resources Research, 49,* 2308-2311. https://doi.org/10.1002/wrcr.20204

Tabari, H., & Willems, P. (2023). Global Risk Assessment of Compound Hot-Dry Events in the Context of Future Climate Change and Socioeconomic Factors. *NPJ Climate and Atmospheric Science, 6,* Article No. 74. https://doi.org/10.1038/s41612-023-00401-7

Trenberth, K. E. (1997). The Definition of El Niño. *Bulletin of the American Meteorological Society, 78,* 2771-2777. https://doi.org/10.1175/1520-0477(1997)078<2771:tdoeno>2.0.co;2

Wilks, D. S. (2011). *Statistical Methods in the Atmospheric Sciences* (3rd ed.). Academic Press.

Zhang, Y., Hao, Z., Feng, S., Zhang, X., & Hao, F. (2023). Changed Relationship between Compound Dry-Hot Events and ENSO at the Global Scale. *Journal of Hydrology, 621,* Article ID: 129559. https://doi.org/10.1016/j.jhydrol.2023.129559